ARTICLE

Aggregation of Organic Dyes on TiO_2 in Dye-Sensitized Solar Cells Models: An *ab Initio* Investigation

Mariachiara Pastore[†,‡] and Filippo De Angelis[†,*]

[†]Istituto CNR di Scienze e Tecnologie Molecolari c/o Dipartimento di Chimica, Università di Perugia, I-06123, Perugia, Italy, and [‡]Istituto Superiore Universitario di Formazione Interdisciplinare Sez. Nanoscienze, Università del Salento, Distretto Tecnologico, *via* Arnesano 16, 73100 Lecce, Italy

ABSTRACT A density functional theory (DFT), time-dependent DFT, and *ab initio* second order Møller—Plesset perturbation theory study of the aggregation of the metal free indoline D102 and D149 dyes on extended TiO_2 models is reported. By selecting the relevant dimeric arrangements on the TiO_2 surface and evaluating, at the same time, the associated spectroscopic response, an almost quantitative description of the extremely different aggregation behavior of the two dyes is provided. Nicely reproducing the experimental evidence, the present results predict strong aggregation interactions and a sizable red-shift of the absorption band in the case of D102, while negligible effects for D149. Our results open the possibility of computationally screening the various aggregation patterns and predicting the corresponding optical response, thus paving the way to an effective molecular engineering of further enhanced sensitizers for solar cell applications.

KEYWORDS: DSSCs · organic dyes · aggregation · D102 · D149 · TiO_2 models · DFT · TDDFT

Owing to the growing renewable energy demand, dye-sensitized solar cells (DSSCs), put forward by O'Regan and Grätzel in 1991,[1,2] have attracted a significant attention as potential low-cost photovoltaic devices. Ru(II) complexes have maintained a clear lead when employed in DSSCs, with highest photon-to-current conversion efficiencies exceeding 11%.[2,3] A great deal of promising metal-free dyes[4−7] have more recently been developed for DSSC applications as alternatives to the costly and nonenvironmentally friendly metal complexes. The great structural variety of the organic dyes, allowing for an effective tuning of the electronic and optical properties, their high molar extinction coefficients, and, above all, their simpler and lower-cost preparation processes with respect to Ru complexes, make these sensitizers an appealing choice in view of large-scale industrial applications. Most notably, top organic dyes currently deliver only slightly lower efficiencies when employed in DSSC compared to Ru(II) dyes, with record efficiencies up to 9%.[8]

The sensitizer performances are strongly affected by some key factors which govern the efficiency of the electron injection into the TiO_2 conduction band,[9] such as the excited state redox potential, the unidirectional electron flow from the donor moiety to the anchoring acceptor group, enhanced by the conjugation across the linker, and the electronic coupling between the lowest unoccupied molecular orbital (LUMO) and the TiO_2 conduction band. Moreover, other factors which play a prominent role in determining the conversion efficiencies, and which are probably more difficult to control, are the charge recombination of the injected electrons with the dye or oxidized electrolyte and the formation of dye-aggregates on the TiO_2 surface.[10−14] Dye-aggregation is generally considered an undesired phenomenon in DSSC, leading to reduced IPCE values by virtue of intermolecular excited state quenching.[10,15,16] In some limited cases, however, a controlled aggregation has been proven to enhance the photocurrent generation as a result of the larger spectral window where light is absorbed, possibly combined to an efficient charge transfer from the aggregate excited state to the semiconductor.[11,15,17,18] An appropriate molecular design and the use of an antiaggregation coadsorbent, typically chenodeoxycholic acid (CDCA),[19] can prevent in some measure the dye-aggregation on the nanocrystalline-TiO_2 surface, improving the overall photovoltaic performances.[18] An emblematic case in this respect is represented by two recently developed and highly efficient indoline dyes, referred to as D102[20] and D149,[5] which, despite their very similar molecular structure, show extremely different response to aggregation on TiO_2 and eventually photo-

*Address correspondence to filippo@thch.unipg.it.

Received for review October 29, 2009 and accepted December 10, 2009.

Published online December 18, 2009. 10.1021/nn901518s

voltaic performances. In fact, upon adsorption on the semiconductor electrode, the D102 dye, Figure 1, containing a one-unit rhodanine ring, exhibits a consistent red-shift (by as much as 0.23 eV) and broadening of the absorption peak compared to the solution spectrum,[20] symptomatic of strong aggregation on the surface. On the other hand, D149, Figure 1, having a two-unit rhodanine group, presents only moderate broadening and negligible bathocromic shift (0.07 eV)[5] from the solution spectrum to the TiO_2-adsorbed one. Moreover, DSSC employing the D149 dye, achieved high efficiency with the use of a much lower CDCA content compared to D102.[5]

A deep understanding of the dye-aggregation mechanism on TiO_2 surfaces and of its implications for DSSCs functioning is obviously a very important requisite for the design of new dyes and for a detailed atomistic understanding of the device functioning. Only recently Snaith *et al.* have reported an experimental investigation on the effect of aggregation in DSSC devices based on the D149 dye,[21] while a detailed atomistic description of dye aggregation phenomena relevant to DSSCs is still missing.

We therefore report here a density functional theory (DFT), time-dependent DFT (TDDFT), and second order Møller-Plesset perturbation theory (MP2) investigation on the aggregation of the prototypical D102 and D149 indoline dyes on extended TiO_2 anatase models, with the aim of ascertaining the possible arrangements of surface aggregates for both dyes, evaluating at the same time their impact on the corresponding electronic and optical properties. Thanks to our realistic models and high-level computational set up, we provide evidence of a *different* aggregation motif for D102 and D149 on TiO_2 induced by the presence in the latter of the second rhodanine ring, leading to drastically different optical responses.

RESULTS AND DISCUSSION

We start our analysis by briefly reporting the results for D102 and D149 stand-alone molecules, Figure 1, and adsorbed on the reduced $(TiO_2)_{38}$ cluster, Figure 2. For the deprotonated dyes[22] we calculate lowest excitation energies in ethanol solution of 2.11 and 2.06 eV for D102 and D149, respectively, both transitions being strongly dipole-allowed (oscillator strengths of 0.820 and 0.805, respectively) and corresponding essentially to HOMO−LUMO excitations. This data, although quite underestimated, agrees with the trend of experimental absorption maxima of 2.53 and 2.36 eV for D102 and D149, respectively.[5] The almost rigid red-shift which we calculate with respect to the experiment was found to be due to the level of theory used for geometry optimizations rather than to the *x-c* functional used in TD-DFT, suggesting that the hybrid B3LYP or PBE0[23] functionals, can successfully reproduce the optical properties of the investigated systems, as previously

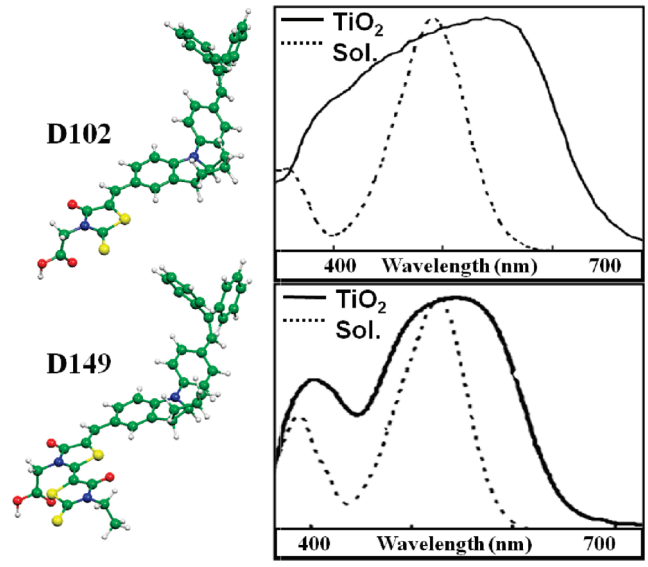

Figure 1. Molecular structures of D102 (upper left) and D149 (lower left); notice, the second rhodanine ring in the molecular structure of D149. Absorption spectra of D102 (upper right) and D149 (lower right) in solution (dashed line) and on TiO_2 (solid line). Upper right graphic reprinted with permission from Horiuchi, T.; Miura, H.; Uchida, S., Highly efficient metal-free organic dyes for dye-sensitized solar cells, *Chem. Commun.* 2003, 3036−3037. Copyright 2003 Royal Society of Chemistry. Lower right graphic adapted from Horiuchi, T.; Miura, H.; Sumioka, K.; Uchida, S., High Efficiency of Dye-Sensitized Solar Cells Based on Metal-Free Indoline Dyes, *J. Am. Chem. Soc.* 2004, *126*, 12218−12219. Copyright 2004 American Chemical Society.

noted.[24,25] This is also confirmed by the fact that when the B3LYP/6-31G* optimized geometries are used, lowest excitations of 2.37 and 2.23 eV are calculated for D102 and D149, respectively, in better agreement with experimental values. We also stress that we are interested here in relative band shifts upon aggregation, rather than in absolutely reproducing excitation energies.

Following previous work on the adsorption of small molecules on anatase TiO_2 (101) surfaces,[26] for D102 we investigated two possible adsorption modes on TiO_2, corresponding to monodentate binding through a single carboxylic oxygen (structure a in Figure 2) and to bidentate binding with proton transfer to a nearby surface oxygen (structure b in Figure 2). As found for related organic dyes,[14,27] we computed the bidentate adsorption mode to be largely energetically favored compared to the monodentate one, by as much as 30 kcal/mol. Although this value might be overestimated, this data clearly points to a D102 bidentate coordination mode, which in turn implies that the dye molecules are lying almost flat with respect to the surface (structure b in Figure 2), rather than pointing in an orthogonal direction to the surface plane (structure a in Figure 2). We notice that our results are in agreement with a recent investigation by Howie *et al.* on D102 and D149 dyes,[28] which was performed for a bidentate adsorption mode based on calculated and measured dye coverages on titania.

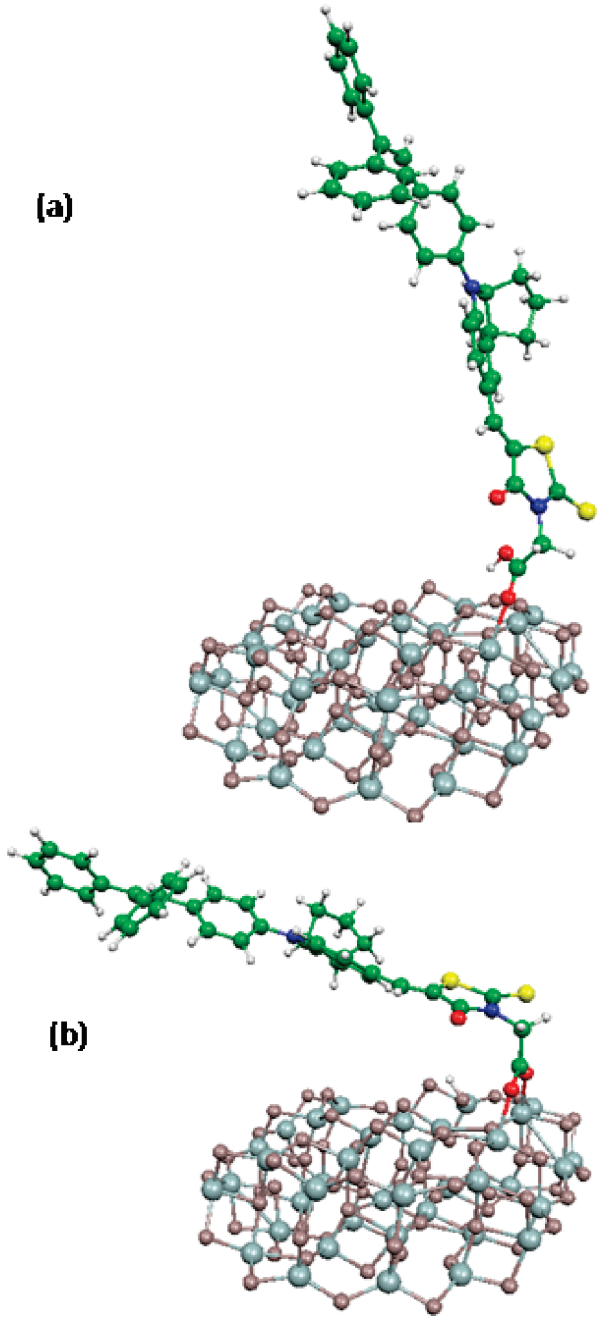

Figure 2. Optimized geometries of the (a) monodentate and (b) bidentate binding modes of D102 on the $(TiO_2)_{32}$ cluster.

Aggregation Schemes. Table 1 compiles the MP2 and B3LYP relative energies of the deprotonated dimers in ethanol solution, computed with respect to the most stable configuration; the description of the nomenclature adopted can be found in the last section, where the model and the computational details are illustrated. An extremely interesting picture comes out from MP2 results: the lowest-energy configuration for D102 is that termed (0,2), having the two molecules aligned along the *y* direction (top of Figure 3) with the π systems almost perfectly stacked. Most notably, this arrangement turns out to be the highest in energy for D149 (by 4.5 kcal/mol), while the preferred configuration is

TABLE 1. B3LYP and MP2 Relative Energies (kcal/mol) of a Series of Dimers of D149 and D102[a]

	D102		D149	
dimer	B3LYP	MP2	B3LYP	MP2
(0,2)	6.80	0.00	12.49	4.50
(2,2)	5.57	3.94	3.23	0.00
(4,2)	0.00	4.47	0.00	3.62
(−2,2)	4.14	4.81	----	----
(4,0)	10.03	1.64	----	----
(−1,1)	11.23	1.23	----	----

[a]The calculations have been carried out on the deprotonated dyes in solution using a 6-31G* basis set. The nomenclature (*x*,*y*) adopted to indicate the position of the second molecule on the TiO_2 surface is illustrated in Figure 5.

(2,2), with the molecules separated by one Ti atom along the *x* axis (bottom of Figure 3). It is also worthwhile to notice that for D102, there are at least two other arrangements, namely (4,0) and (−1,1), precluded to D149 because of the presence of the second rhodanine ring, which are very close in energy to the (0,2) dimer. Moreover, to exclude any artifact due to the solvation effects, we also carried out MP2 calculations on the protonated dimers in gas phase, quantitatively confirming the relative energetic order reported in Table 1.

Using the size-consistent MP2 data, the stability of the aggregates with respect to the noninteracting monomers can be easily estimated as the difference between the energy of the dimer and twice the energy of the isolated molecule at the same level of calculation. For D102, the favored (2,0) dimer is computed to be 9.0 kcal/mol lower in energy than two isolated molecules, while the energy of the more stable (2,2)-D149 configuration is slightly higher (3.2 kcal/mol) than that of two noninteracting D149 molecules. These results clearly account for the experimentally observed different tendency of the two dyes to form aggregates on the TiO_2 surface, predicting a sizable stabilization upon dye-aggregation for D102 while essentially no energy gain in the case of D149. As is also apparent, the energetics obtained by DFT and MP2 are rather different. For both dyes, DFT does not predict dye aggregation, delivering an increasing stability as the distance between the two dye molecules increases: the (4,2) configuration is predicted to be the more stable one for both D102 and D149.

A survey of optimized molecular structures for all possible dimeric arrangements of D102 and D149 on TiO_2 is reported in Supporting Information. Here we briefly discuss the preferred dye dimeric arrangements on TiO_2 and report in Figure 3 the corresponding optimized geometries of (0,2)-D102 and (2,2)-D149. As elsewhere reported for similar dyes,[27] the interaction between the deprotonated molecules and the TiO_2 surface is rather strong, with average calculated distances between the carboxylic oxygens and the TiO_2 surface (O−Ti bond) of 2.05−2.1 Å. In the closest (0,2)-

D102 configuration, the distance between the carboxylic carbons of the two molecules is roughly 10.5 Å, while it amounts to 11.1 Å in the (2,2)-D149 dimer. Moreover, the surface-bound dye molecules lie slightly bent with respect to the TiO_2 surface in both dimeric arrangements, but in the (0,2)-D102 dimer the π systems are perfectly stacked with a reciprocal average distance of about 3.5−4.0 Å.

In summary, on the basis of our model calculations we have identified different aggregation schemes for D102 and D149, which, as we shall discuss in the next section, will arguably have a different impact on the excited states. Intuitively, one can indeed expect a stronger electronic coupling in the π-stacked (2,0)-D102 structure rather than in (2,2)-D149 dimer.

Absorption Spectra. Considering the stability order discussed above, we report in Table 2 the excitation energies and the oscillator strengths of the lowest excited states for the relevant dimeric configurations: (0,2), (4,0) and (−1,1) for D102 and (2,2) for D149. The energy shifts are computed with respect to the lowest excited states of the stand-alone D102 and D149 dyes.

The results show that the different aggregation schemes investigated for D102 have different, and even opposite, effects on the excited states. In fact, the (4,0) configuration with the molecules placed side-by-side and the π-systems almost parallel, produces a blue-shift of the excited states, typical of so-called H-aggregates. If one looks at the excited state with the largest oscillator strength (1.195), located at 2.21 eV, the blue-shift of the absorption maximum for the (4,0) dimer is even more pronounced, amounting to *ca*. 0.1 eV, so that this aggregation pattern can be reasonably disregarded. On the other hand, the two D102 dimeric arrangements which induce a sizable $\pi-\pi$ stacking, (0,2) and (−1,1), imply the appearance of new bands in the absorption spectra which are substantially red-shifted compared to the monomer spectrum (0.15 and 0.11 eV, to be compared to a 0.23 eV experimental shift), a characteristic signature of J-aggregates. Notably, the most stable (0,2) dimer shows also the largest red-shift. Notice also that a comparable excited state evolution accompanies the formation of the (0,2) and (−1,1) dimers, so that on the basis of calculated data alone, it is hardly possible to establish the preferred aggregation motif between these two configurations for D102.

If we now compare the calculated data for D102 and D149, our model almost quantitatively reproduces the different spectroscopic behavior of the two dyes adsorbed on the TiO_2 surface. Selecting the most stable configurations, the red-shifts computed upon aggregation are 0.15 and 0.08 eV for D102 and D149, respectively, to be compared to the experimentally measured

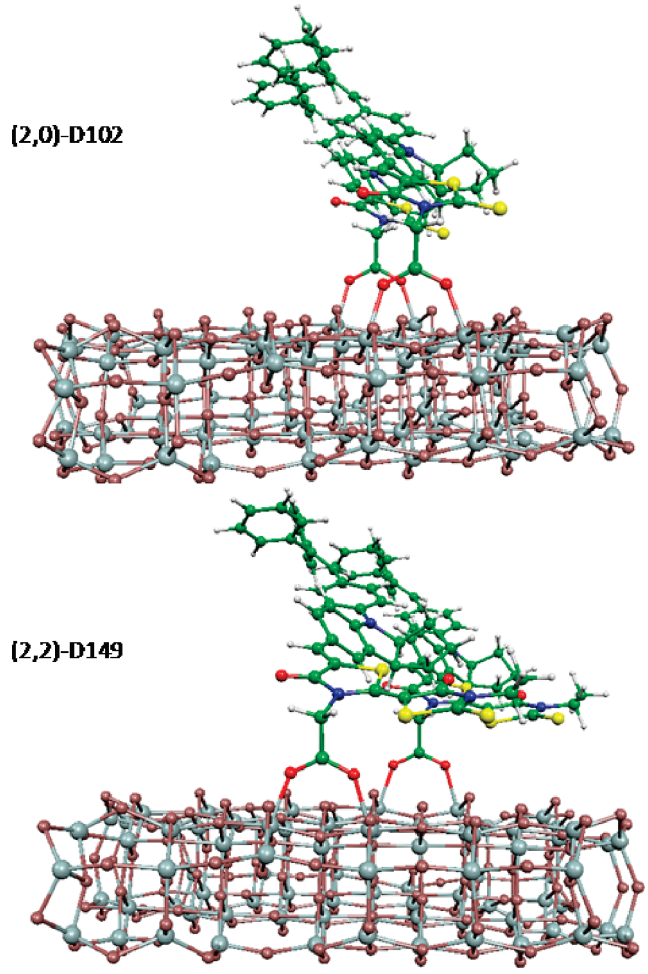

Figure 3. Optimized structures of the preferred (0,2)-D102 (top) and (2,2)-D149 (bottom) configurations.

values of 0.23[20] and 0.07 eV.[5] Most notably, also the computed oscillator strengths for the dimer excited states further reveal a stronger interaction in the case of the (0,2)-D102 configuration, with *ca*. a 3-fold reduction of the J-band oscillator strength calculated in (2,2)-

TABLE 2. Computed TDDFT(B3LYP)/6-31G* Excitation Energies (eV) and Oscillator Strengths for the Four Lowest Excited States of the Most Stable Dimers of D102 and D149.[a]

dimer	excited energy	*F*	shift
(0,2)-D102	1.96	0.022	−0.15
	2.10	1.016	
	2.18	0.537	
	2.28	0.001	
(4,0)-D102	2.13	0.075	+0.02
	2.14	0.077	
	2.21	1.195	
	2.27	0.048	
(−1,1)-D102	2.00	0.028	−0.11
	2.09	0.535	
	2.23	0.698	
	2.30	0.283	
(2,2)-D149	1.97	0.007	−0.08
	2.05	0.720	
	2.07	0.784	
	2.23	0.001	

[a]The corresponding shifts (eV) with respect to the reference monomers are listed in the last column.

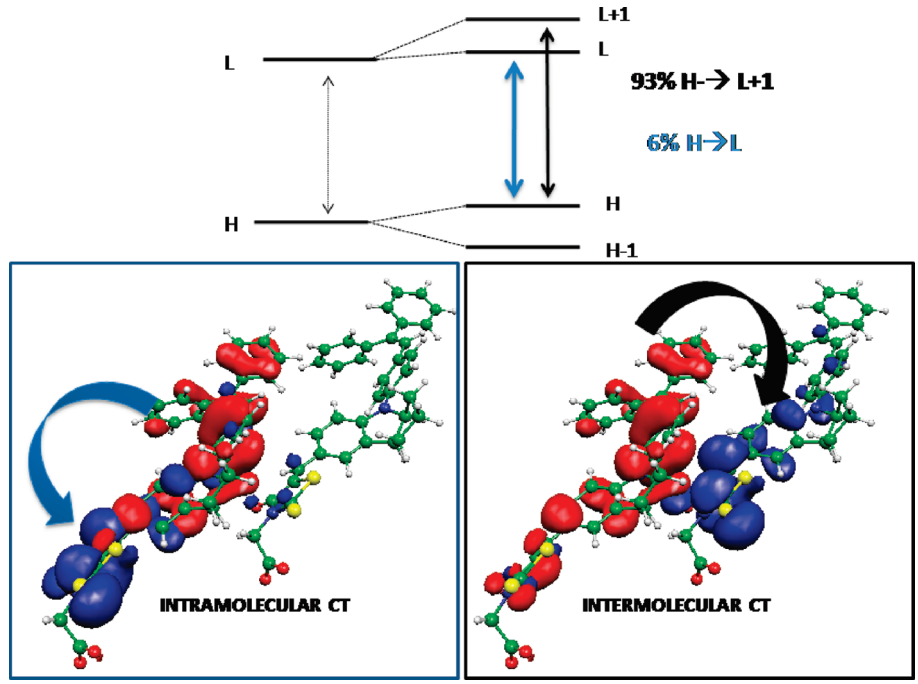

Figure 4. Schematic representation of the HOMO−LUMO splitting in the dimeric (0,2)-D102 configuration. The intramolecular and intermolecular charge transfer (CT) excitations are shown by plotting the electronic density of the HOMO−LUMO transition (intramolecular) and HOMO−LUMO+1 transition (intermolecular).

D149. On overall, the larger shift and higher intensity of the new spectroscopic feature appearing in D102 as a function of dye aggregation is perfectly in line with the available experimental information.

The interaction underlying the optical responses of the favored aggregate configurations are those typical of the formation of J-aggregates.[29] Upon interaction of the molecular orbitals of the two monomeric units, a splitting of the otherwise degenerate highest occupied molecular orbitals (HOMOs) and lowest unoccupied molecular orbitals (LUMOs) occurs, providing a set of two couples of occupied and unoccupied orbitals, see Figure 4 for the D102 case. The red-shifted optical response is the result of intermolecular excitations, which displace electron density from the HOMO, largely based on one monomeric unit, to the LUMO+1, maximally localized on the other monomer, Figure 4. A slight mixing (*ca.* 6%) with the intramolecular CT HOMO → LUMO transition is also found. Obviously, the splitting (therefore the red-shift) and the oscillator strength of the new transitions characterizing the dimeric aggregates strongly depend on the electronic coupling, which, for a given molecular system, decreases with an increase in the distance between the two monomers. This picture nicely accounts for the different behavior of D102 and D149, whereby D149 cannot attain the strongly coupled configurations which in D102 are the energetically preferred ones.

In a further attempt to discriminate between the two possible D102 (0,2) and (−1,1) dimeric configurations, we might resort to available experimental dye coverages, which were conveniently estimated for the same dyes by Howie *et al.*[28] In that work, exactly the

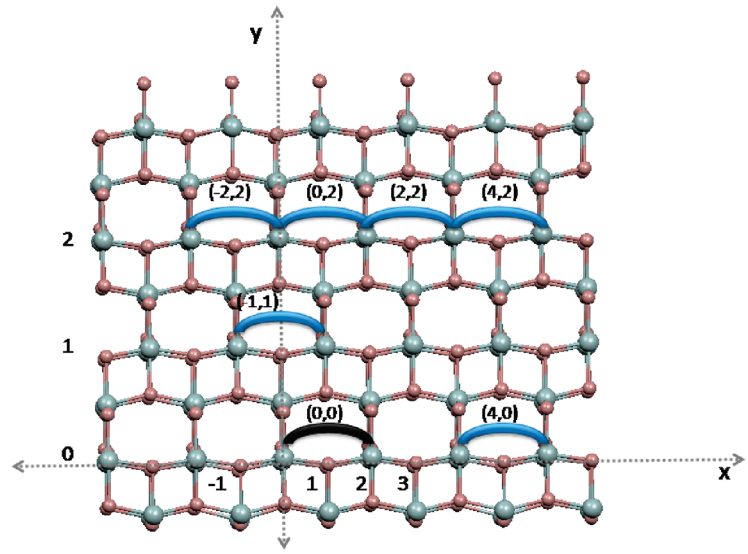

Figure 5. Graphical representation of the (101) $Ti0_2$ anatase surface. The scheme illustrates the convention adopted to indicate the relative positions of two molecules: each couple is labeled with the (*x*,*y*) coordinates of the second molecule, the first one being conventionally fixed in (0,0).

same coverage (3.6×10^{13} cm^{-2}) was measured for both D102 and D149.[28] The favored (0,2)-D102 and (2,2)-D149 configurations produce essentially the same calculated coverage, which incidentally turns out to be of the order of 3.7×10^{13} cm^{-2}, while the closer packing attained by the (−1,2)-D102 dimer results in a higher coverage, of the order of 5×10^{13} cm^{-2}. Therefore, two competing aggregation motifs can be outlined for D102 on the basis of energetics and optical response, while the only configuration compatible with the experimental coverage is (0,2)-D102; in any case, only the (2,2) aggregation configuration seems possible for D149.

CONCLUDING REMARKS

We have presented a computational investigation, based on *ab initio* MP2 and DFT/TDDFT calculations of the aggregation of two metal free indoline dyes, namely D102 and D149, on an extended $(TiO_2)_{82}$ model. Our computational approach, based on a preliminary selection of the relevant preferred dimeric arrangements on the TiO_2 surface and on the subsequent precise evaluation of the associated optical responses, fully accounts for the experimental evidence of a drastically different behavior of the two dyes against aggregation on the semiconductor surface. Briefly, we found different aggregation motifs for the two dyes, showing that in the most stable D102 dimeric arrangement, the dyes molecules lie aligned with the π system perfectly stacked, whereas the preferred configuration for the sterically hindered D149 has the two molecules separated by one Ti atom, thus leading to a reduced $\pi-\pi$ stacking interaction. Excited state calculations on the selected dimers almost quantitatively reproduced the measured red-shifts, predicting values of 0.15 and 0.08 eV for D102 and D149, respectively, to be compared with the experimental values of 0.23 and 0.07 eV, confirming the overall picture extracted from the adsorption studies.

The present results represent a first successful attempt of providing a theoretical model for the complex aggregation phenomena of organic dyes on TiO_2 electrode surfaces. The possibility of discriminating among the various aggregation patterns and predicting the corresponding optical response pave the way to an effective molecular engineering of further enhanced sensitizers for solar cell applications.

MODELS AND COMPUTATIONAL DETAILS

Using a simple topological approach we investigate the aggregation patterns of the D102 and D149 dyes, providing a qualitative and quantitative description of the different optical responses of the dyes adsorbed on the TiO_2 anatase surface. To this end, we employ a TiO_2 nanoparticle model consisting of a (101) $(TiO_2)_{82}$ anatase slab of approximately 4 nm^2 area, with three rows of five- and six-coordinated surface Ti sites and sufficient coordination sites to accommodate the considered dimeric arrangements. On this TiO_2 slab we have investigated the dye-aggregation for both D102 and D149, initially selecting among all the possible dimeric arrangements the closest interacting ones with no explicit superposition of atomic structures. Using a reduced $(TiO_2)_{38}$ model,[30,31] we have investigated both monodentate and bidentate dye binding modes on TiO_2. Even though surface protonation is known to have a large impact on DSSC efficiency,[27] we considered the dyes to be deprotonated in their interaction with the surface, to limit the number of variables of our model. After this preliminary screening, a set of six configurations was selected for D102 (Supporting Information), while, due to the steric hindrance introduced by the presence of the second rhodanine moiety, only three of them were retained as possible candidates for the D149 molecule (Supporting Information). The nomenclature we use to label the dimer confirgurations is illustrated in Figure 5, along with a top view of the anatase TiO_2 (101) surface. Keeping fixed the position of the molecule placed in (0,0), each dimer is labeled by the (x,y) coordinates of the second molecule. Therefore, the six dimers of D102 examined in this study are labeled as (4,0), (−1,1), (−2,2), (0,2), (2,2), and (4,2); for D149 only the (0,2), (2,2), and (4,2) configurations are considered.

For each configuration, the geometries of the dyes adsorbed on the TiO_2 surface have been optimized by the Car−Parrinello (CP) method[32] using the PBE exchange-correlation functional,[33] a plane-wave basis set and ultrasoft pseudopotentials.[34,35] Additional geometry optimizations on the D102 and D149 isolated molecules were performed at the same level of theory employed for the dimers.

To evaluate the relative stability of the various optimized configurations, we carried out single point MP2 as well as DFT calculations on the deprotonated dimers in solution taking the optimized geometries of the dyes adsorbed onto TiO_2. We expect MP2 to provide a reliable description of the energetic underlying the weak (mainly $\pi-\pi$ stacking and van der Waals) interactions responsible for dye aggregation.[36] The absorption spectrum of the D102 and D149 monomers and of each dimeric arrangement was computed by TDDFT with the hybrid B3LYP exchange-correlation functional.[37] Both MP2 and TDDFT calculations were carried out with the 6-31G* basis set, taking into account solvation effects by means of the conductor-like polarizable continuum model (C-PCM)[38,39] as implemented in the Gaussian 03 package.[40] We also checked the consistency of MP2 data on the deprotonated dyes, by performing benchmark calculations *in vacuo* on the protonated species.

Acknowledgment. We thank MIUR (FIRB 2003: Molecular compounds and hybrid nanostructured materials with resonant and nonresonant optical properties for photonic devices) and CNR (PROMO 2006) for financial support.

Supporting Information Available: Optimized molecular structures of the considered D102 and D149 dimers adsorbed on the $(TiO_2)_{82}$ cluster. This material is available free of charge *via* the Internet at http://pubs.acs.org.

REFERENCES AND NOTES

1. O'Regan, B.; Grätzel, M. A Low-Cost, High-Efficiency Solar Cell Based on Dye-Sensitized Colloidal TiO_2 Films. *Nature* **1991**, *353*, 737–740.
2. Nazeeruddin, M. K.; De Angelis, F.; Fantacci, S.; Selloni, A.; Viscardi, G.; Liska, P.; Ito, S.; Takeru, B.; Grätzel, M. Combined Experimental and DFT-TDDFT Computational Study of Photoelectrochemical Cell Ruthenium Sensitizers. *J. Am. Chem. Soc.* **2005**, *127*, 16835–16847.
3. Grätzel, M. Conversion of Sunlight to Electric Power by Nanocrystalline Dye-Sensitized Solar Cells. *J. Photochem. Photobiol., A* **2004**, *164*, 3–14.

4. Hara, K.; Kurashige, M.; Ito, S.; Shinpo, A.; Suga, S.; Sayama, K.; Arakawa, H. Novel Polyene Dyes for Highly Efficient Dye-Sensitized Solar Cells. *Chem. Commun.* **2003**, 252–253.
5. Horiuchi, T.; Miura, H.; Sumioka, K.; Uchida, S. High Efficiency of Dye-Sensitized Solar Cells Based on Metal-Free Indoline Dyes. *J. Am. Chem. Soc.* **2004**, *126*, 12218–12219.
6. Kim, S.; Lee, J. K.; Kang, S. O.; Ko, J.; Yum, J. H.; Fantacci, S.; De Angelis, F.; Di Censo, D.; Nazeeruddin, M. K.; Grätzel, M. Molecular Engineering of Organic Sensitizers for Solar Cell Applications. *J. Am. Chem. Soc.* **2006**, *128*, 16701–16707.
7. Hagberg, D. P.; Edvinsson, T.; Marinado, T.; Boschloo, G.; Hagfeldt, A.; Sun, L. C. A Novel Organic Chromophore for Dye-Sensitized Nanostructured Solar Cells. *Chem. Commun.* **2006**, 2245–2247.
8. Ito, S.; Zakeeruddin, S. M.; Humphry-Baker, R.; Liska, P.; Charvet, R.; Comte, P.; Nazeeruddin, M. K.; Péchy, P.; Takata, M.; Miura, H.; *et al.* High-Efficiency Organic-Dye-Sensitized Solar Cells Controlled by Nanocrystalline−TiO_2 Electrode Thickness. *Adv. Mater.* **2006**, *18*, 1202–1205.
9. Miyashita, M.; Sunahara, K.; Nishikawa, T.; Uemura, Y.; Koumura, N.; Hara, K.; Mori, A.; Abe, T.; Suzuki, E.; Mori, S. Interfacial Electron-Transfer Kinetics in Metal-Free Organic Dye-Sensitized Solar Cells: Combined Effects of Molecular Structure of Dyes and Electrolytes. *J. Am. Chem. Soc.* **2008**, *130*, 17874–17881.
10. Tatay, S.; Haque, S. A.; O'Regan, B.; Durrant, J. R.; Verhees, W. J. H.; Kroon, J. M.; Vidal-Ferran, A.; Gavina, P.; Palomares, E. Kinetic Competition in Liquid Electrolyte and Solid-State Cyanine Dye Sensitized Solar Sells. *J. Mater. Chem.* **2007**, *17*, 3037–3044.
11. Sayama, K.; Tsukagoshi, S.; Hara, K.; Ohga, Y.; Shinpou, A.; Abe, Y.; Suga, S.; Arakawa, H. Photoelectrochemical Properties of J Aggregates of Benzothiazole Merocyanine Dyes on a Nanostructured TiO_2 Film. *J. Phys. Chem. B* **2002**, *106*, 1363–1371.
12. Burfeindt, B.; Hannappel, T.; Storck, W.; Willig, F. Measurement of Temperature-Independent Femtosecond Interfacial Electron Transfer from an Anchored Molecular Electron Donor to a Semiconductor as Acceptor. *J. Phys. Chem.* **1996**, *100*, 16463–16465.
13. Liu, D.; Fessenden, R. W.; Hug, G. L.; Kamat, P. V. Dye Capped Semiconductor Nanoclusters. Role of Back Electron Transfer in the Photosensitization of SnO_2 Nanocrystallites with Cresyl Violet Aggregates. *J. Phys. Chem. B* **1997**, *101*, 2583–2590.
14. Tian, H.; Yang, X.; Chen, R.; Zhang, R.; Hagfeldt, A.; Sun, L. Effect of Different Dye Baths and Dye-Structures on the Performance of Dye-Sensitized Solar Cells Based on Triphenylamine Dyes. *J. Phys. Chem. C* **2008**, *112*, 11023–11033.
15. Ehret, A.; Stuhl, L.; Spitler, M. T. Spectral Sensitization of TiO_2 Nanocrystalline Electrodes with Aggregated Cyanine Dyes. *J. Phys. Chem. B* **2001**, *105*, 9960–9965.
16. Wang, Z.-S.; Cui, Y.; Dan-oh, Y.; Kasada, C.; Shinpo, A.; Hara, K. Thiophene-Functionalized Coumarin Dye for Efficient Dye-Sensitized Solar Cells: Electron Lifetime Improved by Coadsorption of Deoxycholic Acid. *J. Phys. Chem. C* **2007**, *111*, 7224–7230.
17. Kawasaki, M.; Aoyama, S. High Efficiency Photocurrent Generation by Two-Dimensional Mixed J-Aggregates of Cyanine Dyes. *Chem. Commun.* **2004**, 988–989.
18. Khazraji, A. C.; Hotchandani, S.; Das, S.; Kamat, P. V. Controlling Dye (Merocyanine-540) Aggregation on Nanostructured TiO_2 Films. An Organized Assembly Approach for Enhancing the Efficiency of Photosensitization. *J. Phys. Chem. B* **1999**, *103*, 4693–4700.
19. Kay, A.; Grätzel, M. Artificial Photosynthesis. 1. Photosensitization of Titania Solar Cells with Chlorophyll Derivatives and Related Natural Porphyrins. *J. Phys. Chem.* **2002**, *97*, 6272–6277.
20. Horiuchi, T.; Miura, H.; Uchida, S. Highly-Efficient Metal-Free Organic Dyes for Dye-Sensitized Solar Cells. *Chem. Commun.* **2003**, 3036–3037.
21. Snaith, H. J.; Karthikeyan, C. S.; Petrozza, A.; Teuscher, J.; Moser, J. E.; Nazeeruddin, M. K.; Thelakkat, M.; Grätzel, M. High Extinction Coefficient "Antenna" Dye in Solid-State Dye-Sensitized Solar Cells: A Photophysical and Electronic Study. *J. Phys. Chem. C* **2008**, *112*, 7562–7566.
22. Chen, K. F.; Hsu, Y. C.; Wu, Q. Y.; Yeh, M. C. P.; Sun, S. S. Structurally Simple Dipolar Organic Dyes Featuring 1,3-Cyclohexadiene Conjugated Unit for Dye-Sensitized Solar Cells. *Org. Lett.* **2009**, *11*, 377–380.
23. Adamo, C.; Barone, V. Toward Reliable Density Functional Methods Without Adjustable Parameters: The PBE0 Model. *J. Chem. Phys.* **1999**, *110*, 6158–6170.
24. Le Bahers, T.; Pauporté, T.; Scalmani, G.; Adamo, C.; Ciofini, I. A TD-DFT Investigation of Ground and Excited State Properties in Indoline Dyes Used for Dye-Sensitized Solar Cells. *Phys. Chem. Chem. Phys.* **2009**, *11*, 11276–11284.
25. Jose, R.; Kumar, A.; Thavasi, V.; Fujihara, K.; Uchida, S.; Ramakrishna, S. Relationship Between the Molecular Orbital Structure of the Dyes and Photocurrent Density in the Dye-Sensitized Solar Cells. *Appl. Phys. Lett.* **2008**, *93*, 023125.
26. Vittadini, A.; Selloni, A.; Rotzinger, F. P.; Grätzel, M. Formic Acid Adsorption on Dry and Hydrated TiO_2 Anatase (101) Surfaces by DFT Calculations. *J. Phys. Chem. B* **2000**, *104*, 1300–1306.
27. Chen, P.; Yum, J. H.; Angelis, F. D.; Mosconi, E.; Fantacci, S.; Moon, S.-J.; Baker, R. H.; Ko, J.; Nazeeruddin, M. K.; Grätzel, M. High Open-Circuit Voltage Solid-State Dye-Sensitized Solar Cells with Organic Dye. *Nano Lett.* **2009**, *9*, 2487–2492.
28. Howie, W. H.; Claeyssens, F.; Miura, H.; Peter, L. M. Characterization of Solid-State Dye-Sensitized Solar Cells Utilizing High Absorption Coefficient Metal-Free Organic Dyes. *J. Am. Chem. Soc.* **2008**, *130*, 1367–1375.
29. Bredas, J.-L.; Cornil, J.; Beljonne, D.; dos Santos, D. A.; Shuai, Z. Excited-State Electronic Structure of Conjugated Oligomers and Polymers: A Quantum-Chemical Approach to Optical Phenomena. *Acc. Chem. Res.* **1999**, *32*, 267–276.
30. Persson, P.; Bergstrom, R.; Lunell, S. Quantum Chemical Study of Photoinjection Processes in Dye-Sensitized TiO_2 Nanoparticles. *J. Phys. Chem. B* **2000**, *104*, 10348–10351.
31. De Angelis, F.; Tilocca, A.; Selloni, A. Time-Dependent DFT Study of $[Fe(CN)_{(6)}]^{(4-)}$ Sensitization of TiO_2 Nanoparticles. *J. Am. Chem. Soc.* **2004**, *126*, 15024–15025.
32. Car, R.; Parrinello, M. Unified Approach for Molecular Dynamics and Density-Functional Theory. *Phys. Rev. Lett.* **1985**, *55*, 2471–2474.
33. Perdew, J. P.; Burke, K.; Ernzerhof, M. Generalized Gradient Approximation Made Simple. *Phys. Rev. Lett.* **1996**, *77*, 3865–3868.
34. Pasquarello, A.; Laasonen, K.; Car, R.; Lee, C.; Vanderbilt, D. *Ab Initio* Molecular Dynamics for D-Electron Systems: Liquid Copper at 1500 K. *Phys. Rev. Lett.* **1992**, *69*, 1982–1985.
35. Giannozzi, P.; Angelis, F. D.; Car, R. First-Principle Molecular Dynamics with Ultrasoft Pseudopotentials: Parallel Implementation and Application to Extended Bioinorganic Systems. *J. Chem. Phys.* **2004**, *120*, 5903–5915.
36. Zhao, Y.; Truhlar, D. G. Benchmark Databases for Nonbonded Interactions and Their Use To Test Density Functional Theory. *J. Chem. Theor. Comp.* **2005**, *1*, 415–432.
37. Becke, A. D. A New Mixing of Hartree−Fock and Local Density-Functional Theories. *J. Chem. Phys.* **1993**, *98*, 1372–1377.
38. Cossi, M.; Barone, V. Time-Dependent Density Functional Theory for Molecules in Liquid Solutions. *J. Chem. Phys.* **2001**, *115*, 4708–4717.
39. Cossi, M.; Rega, N.; Scalmani, G.; Barone, V. Energies, Structures and Electronic Properties of Molecules in Solution with the C-PCM Solvation Model. *J. Comput. Chem.* **2003**, *24*, 669–681.
40. Frisch, M. J.; Trucks, G. W.; Schlegel, H. B.; Scuseria, G. E.; Robb, M. A.; Cheeseman, J. R.; Montgomery, J. A.; Jr., T. V.; Kudin, K. N.; Burant, J. C.; Millam, J. M.; *et al. Gaussian 03,* revision B05; Gaussian Inc.: Pittsburgh, PA, 2003.